Ambient-based Oscillation Mode Analysis via Dynamic Ensemble ITD and ARMA Model for Converter-based FFR Application

Wei Qiu[1,2], Yuqing Dong[1], Lin Zhu[1], Shutang You[1], Qiu Tang[2], Junfeng Duan[2], Wenxuan Yao[2, 3], Yilu Liu[1,3]
Department of EECS
[1]University of Tennessee, [2]Hunan University, [3]Oak Ridge National Laboratory
Knoxville, USA
{qwei4, ydong22, lzhu12, syou3}@utk.edu, {tangqiu, duanjunfeng}@hnu.edu.cn, ywxhnu@gmail.com, liu@utk.edu

2020 IEEE Student Conference on Electric Machines and Systems (SCEMS) | 978-1-7281-5622-4/20/$31.00 ©2020 IEEE | DOI: 10.1109/SCEMS48876.2020.9352339

***Abstract*—The accuracy of oscillation mode information become an essential reference to large-scale dynamics power system with a high proportion integration of converters. However, the difference in the data trend of the measurement unit will affect the recognition accuracy of the oscillation. To address this problem, this paper first proposes a Dynamic Ensemble Intrinsic Time-Scale Decomposition (DEITD) to remove the data trend. It improves the fitting effect of trends by optimizing the modal aliasing and number of decomposition. Next, the Yule-Walker based Auto Regressive Moving Average (ARMA) technique is utilized to estimate the low frequency oscillation modes. Multiple experiments on simulation and actual signals manifest that the proposed framework has better performance and is more real-time than some conventional methods, which can be used as the control signal of the converter-based fast frequency reserve to enhance the system stability.**

***Index Terms*—Auto Regressive Moving Average, Dynamic Ensemble ITD, Oscillation modes, Ambient data**

I. Introduction

With the increasing number of the converter integrating into the power system, the system inertia witnessness continuous decreasing recently [1]. Conventional response reserve may be insufficient for following detailed dynamic manifestations of power systems. Meanwhile, the low frequency oscillation with a frequency range of 0.1 to 2.5 Hz, is the active power oscillation on the power transmission line [2], [3]. It can damage the stability of power system when the oscillation occurs because the transmission capacity will be limited [4], [5]. Thereby, the oscillation estimation is of paramount important for the power system control [6], [7], and the estimated results of ambient data can potentially be used for the converter-based fast frequency response application. Once started, it may continue for a while and cause power system collapse. Importantly, the effect of Power System Stabilizer (PSS) will be reduced if the oscillation modes are not accurately measured, as the parameter of PSS is primarily based on the modal analysis [8]. Therefore, it is essential to develop methods to accurately estimate the parameters of low frequency oscillation.

Generally, the modal estimation methods can be performed based on two types of approaches, including the system based and data driven based methods [9]. The system based approach linearizes the system function through theoretical derivation. For example, the linear rotor motion equation is used to analyze the features of generator kinetic [10]. However, this method cannot be applied to modal analysis once the system structure changes and the system model is no longer valid.

To solve the above issue, different data-driven based methods are proposed. The Prony is one of the most commonly used methods to calculate the oscillation parameters [10]. However, it suffers from the measurement and ambient noise when the Signal-to-Noise Ratio (SNR) is lower than 30dB due to the lower noise immunity. Some other methods, including the matrix pencil [11], Empirical Mode Decomposition (EMD) and Hilbert transform [12], also have been successfully applied to modal estimation. Nevertheless, the estimation accuracy can decrease if the parameters of EMD has not been properly tuned. The Auto Regressive Moving Average (ARMA) model has been proved effective for detecting oscillations even using the ambient data [9]. Since the event signal of the system is difficult to obtain, the oscillation parameters of the ambient data become one of the basis of the power system control. However, the slow trend (DC trend) in the ambient data is difficult to be eliminated and the leaked energy affects the estimated result.

To reduce the impact of the DC trend, the Intrinsic Time-Scale Decomposition (ITD) method can be used to decompose a non-stationary signal into multiple sub-signals and residual trend signal [13]. Therefore, useful effective information is expected to be extracted by removing the DC component. However, it has two practical limitations that reduce its application in processing the oscillation mode analysis. The first is that the trend component is difficult to be accurately identified, resulting in the leakage of oscillation energy. The second is that difference in the number of decomposition in ITD will cause errors.

Therefore, this paper proposes a Dynamic Ensemble Intrinsic Time-Scale Decomposition (DEITD) to accurately eliminate the slow trend items. Combined with the advantages of ARMA's high accuracy, a novel oscillation estimation method is proposed based on DEITD and ARMA.

II. Detrending using DEITD

Due to the dynamic changes of the power system, including load and power output adjustment, the measurement data of the power system is changeable and non-linear. The non-linear trend of the measurement data will reduce the effect of oscillation recognition if it is not accurately removed. To eliminate this, an

This work is supported by the Engineering Research Center Program of the National Science Foundation and DOE under NSF Award Number EEC-1041877, the CURENT Industry Partnership Program, and the Postgraduate Scientific Research Innovation Project of Hunan Province.

adaptive decomposition method DEITD is proposed to remove the non-linear trend. Compared with the traditional detrending methods, including the EMD and polynomial fitting methods [14], the advantages of DEITD are that it is more real-time and has more precise detrending results.

A. Procedure of ITD

Given the measurement data as x_t, where the x_t can be frequency, angle, and power data. In the ITD, the x_t can be expressed as the sum of baseline and proper rotation signal.

$$x_t = \Upsilon x_t + (1-\Upsilon)x_t = R_t + H_t \tag{1}$$

where Υ is the baseline-extracting operation to extract the oscillation modes, the $R_t = \Upsilon x_t$ denotes the baseline signal, namely the object trend component which needs to be removed. H_t denotes the proper rotation.

To obtain the R_t, the local extrema of x_t is denoted as τ_k, where $k = 1, 2, ...$ The first point τ_k is set to $\tau_0 = 0$ for convenience. When $t \in [0, \tau_{k+2}]$, the operation Υ on the interval $(\tau_k, \tau_k + 1]$ can then be defined as

$$\Upsilon x_t = R_k + \left(\frac{R_{k+1} - R_k}{x_{k+1} - x_k}\right)(x_t - x_k), t \in (\tau_k, \tau_k + 1] \tag{2}$$

where $R_0 = (x_{\tau_0} + x_{\tau_1})/2$. The R_{k+1} is the function related to τ_k, where the definition can be derived from [13]. The baseline signal Υx_t is a linearly transformed contraction to make the proper rotations monotonic between extrema.

For the complex oscillation signal, the process can be re-applied for p times using the generated R_t to complete ITD decomposition, which can be calculated as

$$\begin{aligned} x_t &= Hx_t + \Upsilon x_t = Hx_t + (H+\Upsilon)\Upsilon x_t \\ &= \big(H(1+\Upsilon) + \Upsilon^2\big)x_t = \big(H\sum_{k=0}^{p-1}\Upsilon^k + \Upsilon^p\big)x_t \end{aligned} \tag{3}$$

where H is the proper-rotation-extracting operator, $H + \Upsilon = 1$, the $H\Upsilon^k x_t$ is the $(k+1)$st level proper rotation, the second item $\Upsilon^p x_t$ is the extracted trend of oscillation signal.

B. Detrending analysis using DEITD

The motivation of DEITD is to obtain an accurate trend component. In the proposed DEITD, the ensemble ITD is utilized to reduce the modal aliasing. It means that N numbers of ITDs are calculated and the results are averaged. Meanwhile, the number of decomposition is automatically determined using the proposed error criteria. The primary steps of DEITD for processing the oscillation signals are as below.

1) *Dynamic selection the number of decomposi−tions p using error criteria.* In DEITD, the p is optimized selected using the Mean Absolute Percentage Error (MAPE) and Root Mean Squared Error (RMSE). The sum of RMSE and MAPE for the detrending signal are calculated using different p in single ITD. The p value with the lowest RMSE and MAPE is selected.
2) *Add white noise.* Different from the ITD, the white noise with standard deviation n_s is first added to oscillation signal x_t to construct a noisy signal. The input of DEITD becomes $x_t + n_w$. The purpose of adding white noise is to smooth pulse interference and reduce modal aliasing through the integration of multiple ITDs [15]. Then, perform the ITD for the noise signal $x_t + n_w$.

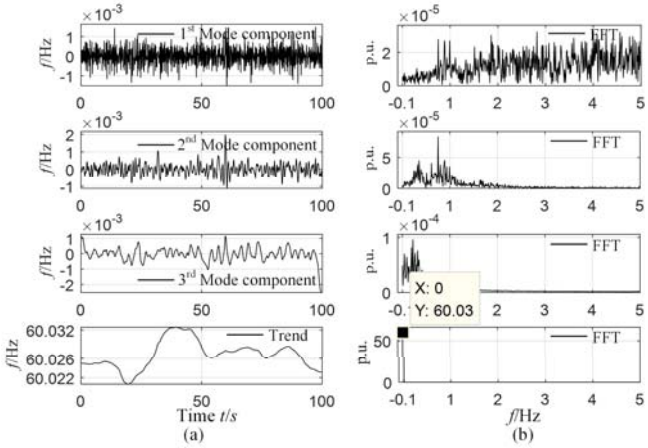

Fig. 1. The decomposition results using DEITD and the corresponding FFT results. (a) The results of DEITD, (b) The FFT of the (a).

3) *Integrate N ITDs and remove the trend.* At this stage, the output of DEITD is obtained by averaging each output of ITD. Denoting the trend output of DEITD as $\Upsilon_e^p(x_t + n_w)$. The trend component can then be removed. The target signal $\bar{x}_t$ can be expressed as $\bar{x}_t = x_t - \Upsilon_e^p(x_t + n_w)$.

In the first step of DEITD, the RMSE and MAPE are used to measure the error of the trend term. Usually, a trend with a better fitting effect should have a smaller error. Therefore, the p can be dynamically selected as

$$p = \text{Index}\{Min(e_{RMSE} + e_{MAPE})\} \tag{4}$$

where the defination of e_{RMSE} and e_{MAPE} are

$$\begin{aligned} e_{RMSE} &= \sqrt{\sum_{i=1}^{n}\big(x_t - \Upsilon_e^p(x_t + n_w)\big)^2} \\ e_{MAPE} &= \frac{1}{n}\sum_{i=1}^{n}\left|\frac{x_t - \Upsilon_e^p(x_t + n_w)}{x_t}\right| \end{aligned} \tag{5}$$

where n is the length of x_t. In this paper, the p is selected from the empirical data set [3, 7] with step size 1. The equation (4) means that the p can be set to the minimum value index of error. In equation (5), the use of two evaluation indicators is to evaluate the trend effect from different aspects.

C. Parameter sensitivity analysis

To illustrate the parameter selection procedure and analyzing the performance of DEITD, an example of ambient frequency data is used. A 100-second ambient data with 10 Hz reporting rate is used. The DEITD results and the corresponding Fast Fourier Transform (FFT) results are shown in Fig. 1, the p is set to 4 here. According to the amplitude spectrum of FFT, the frequency components have been divided into different intervals for the 1^{st} to 3^{rd} mode components. Particularly, the FFT of the trend component only contains the DC frequency, indicating that the trend of ambient data has been successfully extracted.

Based on the step (1) of DEITD, the p is first selected using the error criteria. Furthermore, the trend of ambient data of three p models with small errors are presented in Fig. 2. Compared with ITD, it shows that the DEITD can fit the ambient data more precisely when $p = 4$ because only 0.0016 error is obtained. However, the DEITD get a smoother trend when $p = 5$ in DEITD. This is because the trend component is split into multiple proper rotation components.

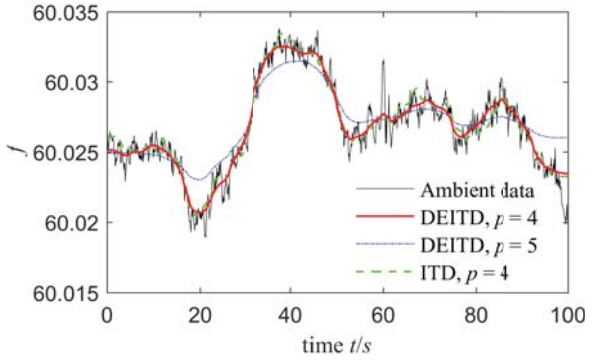

Fig. 2. The detrending performance with different p. The sum of $e_{RMSE}+e_{MAPE}$ errors are 0.0016, 0.0035, and 0.0021 for the DEITD ($p = 4$, $p = 5$), and ITD, respectively.

III. Yule-Walker based ARMA Model

After the trend is removed, the mode parameter estimation method is developed to accurately identify the oscillation. An ARMA process technique is used, where the AR parameters are calculated using the Yule-Walker (YW) method. The advantages of the YW based ARMA are that it is robust to both ring-down and ambient signals.

The ARMA process can be seen as two processes of AR and MA parts, which can be expressed as

$$\bar{x}_t = \sum_{i=1}^{h} \varphi_i \bar{x}_{t-i} - \sum_{i=1}^{m} \theta_i u_{t-i} \tag{6}$$

where φ_i is the coefficients of AR part, which captures the observed mode information including the frequency and damping ratio. θ_i is the coefficients of MA part, it captures the influence of controls. u_t denotes the white noise, which represents the load changes in system.

To obtain the oscillation modes, the pole coefficients φ_i should be derived. To solve this problem, the YW method is used which based on the autocorrelation function of $\bar{x}_t$. The autocorrelation function can be given as

$$r_k = \frac{1}{n} \sum_{i=k+1}^{n} \bar{x}_i \bar{x}_{i-k} \tag{7}$$

In ARMA model, the following relation can be satisfied

$$r_k = -\sum_{i=1}^{h} \varphi_i r_{k-i}, \ k \geq h \tag{8}$$

The pole coefficients φ_i can be calculated using the following equations

$$\begin{bmatrix} r_{m+1} \\ r_{m+2} \\ \vdots \\ r_{m+M} \end{bmatrix} = \begin{bmatrix} r_m & r_{m-1} & \cdots r_{m-h+1} \\ r_{m+1} & r_m & \cdots r_{m-h+2} \\ \vdots & \vdots & \vdots & \vdots \\ r_{m+M-1} r_{m+M-2} \cdots & & r_m \end{bmatrix} \begin{bmatrix} \varphi_1 \\ \varphi_2 \\ \vdots \\ \varphi_h \end{bmatrix} \tag{9}$$

where $M \geq h$. The equation (9) is called the YW equation. Then the estimated mode can be obtained from the root of the following polynomial.

$$\lambda^h + \sum\nolimits_{i=1}^{h} \varphi_i \lambda^{h-i} = 0 \tag{10}$$

Denoting its root as λ_i, the frequency and damping ratio can be calculated through solving equation (11)

$$f_i = \frac{f_s}{2\pi} |ln(\lambda_i)|, \ d_i = \frac{-Re\{ln(\lambda_i)\}}{|ln(\lambda_i)|} \tag{11}$$

where f_s is the sampling rate of x_t. The amplitude and phase of oscillation mode can be derived using the Vandermonde matrix and Total Least-Squares (TLS) technique in [16].

A. Parameter selection and result evaluation

The accuracy of oscillation results are affected by the parameters of ARMA, including the parameters h and m. To select the suitable parameters, the Akaike Information Criterion (AIC) and Bayesian Information Criterion (BIC) are used. Generally, the lower AIC and BIC value mean a better ARMA model. According to the lowest AIC and BIC values, different parameters h and m are tested using the ambient data to determine the final parameters.

Meanwhile, to evaluate the accuracy of the results, the SNR is used [17], which can be derived as

$$SNR = 10log \frac{\sum_{i=0}^{n-1} x_t^2[i]}{\sum_{i=0}^{n-1} (x_t[i] - \hat{x_t}[i])^2} \tag{12}$$

where $\hat{x_t}$ is the fitting values of x_t based on the estimated parameters. Generally, a higher SNR value denotes the better result.

IV. Oscillation Analysis Framework

Based on the proposed DEITD and ARMA models, this section proposes a framework called DEITD-ARMA for the oscillation mode analysis. The flowchart is shown in Fig. 3. It is clear that the DEITD-ARMA can be divided into two parts:

1) Detrend analysis: The trend of the ambient or the ring-down data is detected by DEITD. Then the trend is obtained from the baseline signal. The detrend is finished by removing the trend from input data x_t. The object oscillation signal is obtained as $\bar{x}_t$.
2) Oscillation mode recognition: The $\bar{x}_t$ is fed into ARMA, the YW method is utilized to calculate the pole. Then the parameters of oscillation modes can be developed.

After that, the proposed framework DEITD-ARMA is evaluated by simulation and actual data experiments.

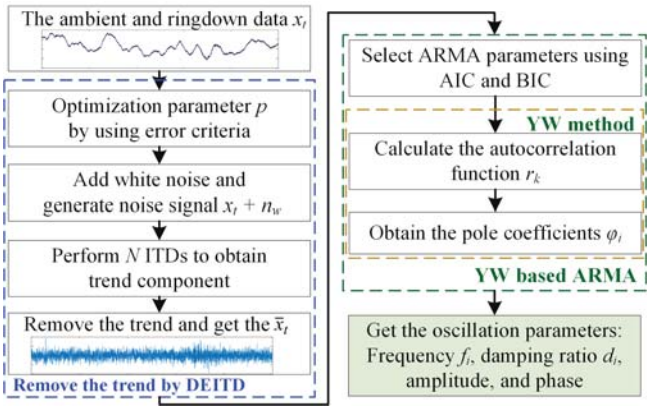

Fig. 3. Oscillation mode analysis framework of ambient data using DEITD-ARMA.

V. Experiment Analysis

To verify the effectiveness of the proposed DEITD-ARMA, different experiments are conducted including the simulation signal, two-area, four generator testing system, and ambient data from FNET/GridEye server. Particularly, the ring-down data is also used to verify the effectiveness of the proposed method. To ensure data consistency, the sampling rate is set to 10 Hz. For the ambient data, the 10 minutes window size is used.

A. Simulations results

The simulation numerical model is

$$x_t = \sum\nolimits_{i=1}^{I} A_i e^{(\sigma_i t)} sin(w_i t + a_{0i}) + x_{tre} + \varepsilon \tag{13}$$

TABLE I
RESULTS COMPARISON USING SIMULATION SIGNALS

Models	Estimation parameters			
	f_0	$d_0(\%)$	f_1	$d_1(\%)$
$Benchmark$	0.2000	19.51	0.8000	2.980
EMD-ARMA	0.2106	24.75	0.7997	3.031
Filter-ARMA	0.1974	**19.46**	0.7999	3.055
ITD-ARMA	0.2028	19.79	0.7993	3.068
Prony [18]	0.2105	13.09	0.8021	3.061
Matrix-pencil [19]	-	-	**0.8001**	13.39
DEITD-ARMA	**0.1998**	19.11	0.7996	**3.024**

where $A_i, \sigma_i, w_i, a_{0i}$ are the amplitude, attenuation factor, angular frequency, and phase angle, respectively. The trend x_{tre} and noise ε are also added to simulate the true low frequency oscillation signal.

In this case, two different modes are designed, of which the signal is shown in Fig. 4. Here, the EMD method is compared with the DEITD. It shows that EMD has a greater fluctuation especially between 20 to 40 s. The benchmark parameters and the estimated results are listed in Table. I. The parameters $A_i, \sigma_i, w_i, a_{0i}$ of these two modes are $\{2.0, -0.25, 0.4\pi, \pi\}$ and $\{1.5, -0.15, 1.6\pi, \pi/2\}$. The damping ratio of these two modes are 19.51% and 2.98%, respectively. The 30 dB white Gaussian noise is superimposed to simulate signal scenarios. The parameters of DEITD-ARMA are set to $p = 4, n_s = 0.5,$ and $N = 30$.

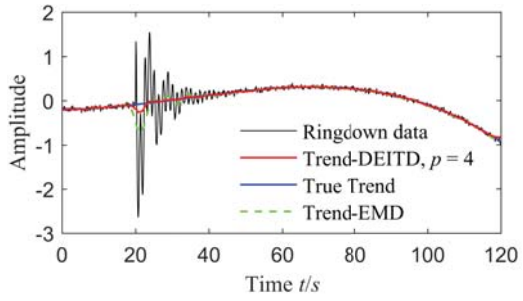

Fig. 4. Simulation low frequency oscillations with two different modes.

As can be seen from Table I, the performance of EMD and ITD based detrend methods obtain lower accuracy. The EMD-ARMA model has more than 0.01 Hz and 5.24% damping ratio absolute errors for f_0 and d_0. A high-pass filter with a cutoff frequency of 0.1 Hz is used (Filter-ARMA). Competitive results are shown for Filter-ARMA. However, the accuracy of f_0 and d_1 has lower performance. The Prony method [18] is sensitive to the noise so low accuracy results are obtained. Moreover, it shows that only one mode is estimated using Matrix-pencil [19]. Compared with other methods, the proposed DEITD-ARMA reaches the highest accuracy even under 30 dB noise, where the maximum absolute error of the frequency and damping ratio is 0.0004 Hz and 0.044%.

B. Simulations on two-area, four generator IEEE system

A typical IEEE testing system of a two-area, four generator power system is shown in Fig. 5. Both areas of the IEEE system include a synchronous generator with a rated power of 900MW. The main parameters can be found in [20].

To identify the oscillation mode of the system, the input is selected as a short-circuit fault on the AC tie

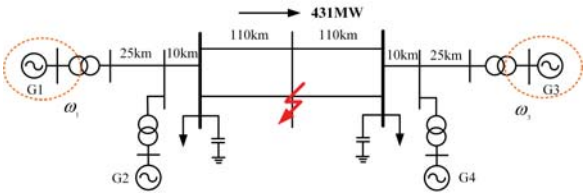

Fig. 5. Configuration of a two-area, four-generator IEEE system.

TABLE II
RESULTS COMPARISON USING SIMULATION SIGNALS

Methods	Estimation parameters			
	f_0	$d_0(\%)$	f_1	$d_1(\%)$
$Benchmark$	0.649	4.63	1.0730	6.53
Prony [18]	0.6553	4.68	1.1661	10.08
Matrix-pencil [19]	0.6584	2.15	1.1277	6.19
DEITD-ARMA	0.6518	4.50	1.1808	6.39

line, which can be regarded as an impulse function since the disturbance time is relatively short (1ms). The output can be chosen as the rotor speed difference between generator G1 and G3. A set of 30-second data with 10 Hz sampling rate is collected from Matlab/Simulink. The linear analysis tool is used to calculate the benchmark oscillation frequency and damping ratio.

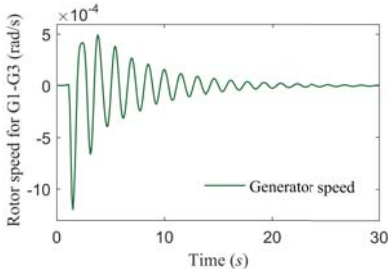

Fig. 6. Inter-area oscillation in two-area, four-generator IEEE system.

The rotor speed signal is shown in Fig. 6, while the identified oscillation modes are listed in Table. II. It can be seen that there are two low frequencies in this two-area, four-generator IEEE system. It shows that the damping ratio of Prony and matrix-pencil is not accuracy, in which the absolute errors are 2.15% and 3.55% for the f_0 and f_1, respectively. Overall, both damping ratio of these two modes are accurate for ARMA models. The two-area, four-generator IEEE system simulation indicates that the ARMA model has better effect even for multiple oscillation modes.

C. Results using ambient data

In this section, the ambient data is used to test the stability and performance of the proposed method. Specifically, the actual frequency data of two PMUs (Units 798 and 966) are collected from the Western Interconnection (WECC) system [21]. The data is collected on October 4-5, 2019. To analyze the stability, the oscillation estimation results are calculated using the data in two days. The window size is 10 min and the step size is set to 5 min. The parameters of DEITD-ARMA are set to $p = 3, n_w = 0.5, N = 30, h = 26,$ and $m = 26$.

To verify the effectiveness of DEITD, the residual characteristics of the detrending data is analyzed first. The ambient data, the detrending data, and the residual test of the detrending data are presented in Fig. 7. According to Fig. 7 (a) and (b), the DC trend component has been removed successfully. The residual test result demonstrates

that useful information has been obtained by ARMA model because the distribution is an approximately normal distribution.

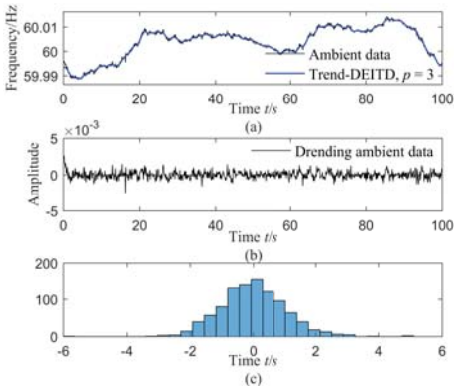

Fig. 7. The residual test of the ambient data.(a)A 100 seconds frequency ambient data. (b) The derending data of (a). (c) The standardized residual test of (b).

The estimated oscillation results of the ambient data are presented in Fig. 8 and 9. The mean and standard deviation are provided. In this two figures, the frequency modes are artificially divided into three intervals including $[0.1-0.3\text{Hz}) \in f_1$, $[0.3-0.5\text{Hz}) \in f_2$, and $[0.5-0.9\text{Hz}] \in f_3$, and marked with different colors for easy observation.

It is obvious that there are three primary frequency components in both units. The frequency components are more accurate than the damping ratio based on the (a) and (b). In Fig. 8 (b), the calculated standard deviations of damping d_1, d_2, d_3 are 25.75%, 21.83%, and 54.06%, respectively. It shows that the standard deviation of the damping ratio is higher than frequency components. This reason is that the damping ratio is related to some factors, including attenuation factor, angular frequency, and noise. The mean results of (a), (b) from Fig. 8 and 9 also show that the oscillation parameters are similar in the two units, indicating the robustness of the method. It should be emphasized that when the damping is higher, it also has a high variability. This also would be one of the characteristics of using ambient data for oscillation analysis. Interestingly, it is found that the frequency is higher at daytime, and the oscillation is lower during the work-time, as shown in Fig. 9. This is related to some new energy equipment and power loads in WECC which may works at daytime. The estimated frequency components are very close to those reported in [22]. The damping ratio is relatively high because the ambient data is used here, where the event data is used in [22].

As can be seen from Fig. 8(c) and Fig. 9(c), it is difficult to determine the dominant frequency because the amplitude are similar for f_1 and f_2. The amplitude of f_3 is much lower, indicating this component is more random. Overall, it means that the proposed DEITD-ARMA is suitable for the online low frequency oscillation analysis.

To verify the accuracy of the results, the SNR is calculated based on equation (12) [23], as shown in Fig. 10. According to equation (12), a better fitting result corresponds to a larger SNR value. Usually, if the value of SNR is over 10 dB, then it indicates that the oscillation results are accurate [23]. The results show that about 15 dB SNR is presented for units 798 and 966, indicating the effectiveness of the DEITD-ARMA.

VI. Conclusions

In this paper, a dynamic ensemble ITD and YW based ARMA model is proposed to automatically estimate the low frequency oscillation from the ambient data. The trend of the ambient data has been removed by optimizing the decomposition components in DEITD. The experimental results show that the DEITD has a better trend fitting effect compared with conventional decomposition methods (such as EMD and ITD). Thereafter, the detrending oscillation signal is estimated by the YW based ARMA model. Simulation results verify that the ARMA has a better estimation accuracy than the Prony and matrix-pencil methods. Different experiments using the simulation and ambient data are conducted to verify the proposed DEITD-ARMA. Finally, the stability and real-time performance have been verified by using the ambient data from two PMU units in the WECC system. Further work will focuses on reducing the effect of noise on the oscillation detection.

References

[1] W. Wang, K. Sun, C. Chen, and et al, "Advanced synchrophasor-based application for potential distributed energy resources management: Key technology, challenge and vision," in *2020 IEEE/IAS Industrial and Commercial Power System Asia (I CPS Asia)*, pp. 1120–1124, 2020.

[2] H. Wang and W. Du, *Analysis and Damping Control of Power System Low-Frequency Oscillations, New York, NY, USA*. Springer, 2016.

[3] W. Wang, C. Chen, L. Zhu, and et al, "Model-less source location for forced oscillation based on synchrophasor and moving fast fourier transformation," in *2020 IEEE PES Innovative Smart Grid Technologies Europe (ISGT-Europe)*, pp. 404–408, 2020.

[4] W. Qiu, Q. Tang, J. Liu, and W. Yao, "An automatic identification framework for complex power quality disturbances based on multifusion convolutional neural network," *IEEE Transactions on Industrial Informatics*, vol. 16, no. 5, pp. 3233–3241, 2020.

[5] W. Qiu, Q. Tang, J. Liu, and et al, "Power quality disturbances recognition using modified s transform and parallel stack sparse auto-encoder," *Electric Power Systems Research*, vol. 174, p. 105876, 2019.

[6] R. K. V. et al, "Simultaneous fast frequency control and power oscillation damping by utilizing pv solar system as pv-statcom," *IEEE Transactions on Sustainable Energy*, vol. 11, no. 1, pp. 415–425, 2020.

[7] W. W. et al, "Information and communication infrastructures in modern wide-area systems," *Wide Area Power Systems Stability, Protection, and Security, Springer*, pp. 71–104, 2020.

[8] A. Q. Zhang, L. L. Zhang, and et al, "Identification of dominant low frequency oscillation modes based on blind source separation," *IEEE Transactions on Power Systems*, vol. 32, no. 6, pp. 4774–4782, 2017.

[9] C. Wu, C. Lu, and et al, "Ambient signals based power system oscillation modes identification considering model order selection," in *2009 IEEE Power Energy Society General Meeting*, pp. 1–7, 2009.

[10] T. Xia, Z. Yu, and et al, "Oscillation energy analysis of inter-area low-frequency oscillations in power systems," *IEEE Transactions on Power Systems*, vol. 31, no. 2, pp. 1195–1203, 2016.

[11] J. Guo, Y. Ye, Y. Zhang, and et al, "Events associated power system oscillations observation based on distribution-level phasor measurements," in *2014 IEEE PES T D Conference and Exposition*, pp. 1–5, 2014.

[12] D. S. Laila, M. Larsson, and et al, "Nonlinear damping computation and envelope detection using hilbert transform and its application to power systems wide area monitoring," in *2009 IEEE Power Energy Society General Meeting*, pp. 1–7, 2009.

[13] M. G. Frei and I. Osorio, "Intrinsic time-scale decomposition: time-frequency-energy analysis and real-time filtering of non-stationary signals," *Proceedings of the Royal Society A: Mathematical, Physical and Engineering Sciences*, vol. 463, no. 2078, pp. 321–342, 2007.

[14] W. Qiu, Q. Tang, K. Zhu, W. Yao, J. Ma, and Y. Liu, "Cyber spoofing detection for grid distributed synchrophasor using dynamic dual-kernel svm," *IEEE Transactions on Smart Grid*, pp. 1–1, 2020.

[15] T. Wang, M. Zhang, Q. Yu, and H. Zhang, "Comparing the applications of emd and eemd on timefrequency analysis of seismic signal," *Journal of Applied Geophysics*, vol. 83, pp. 29 – 34, 2012.

[16] A. Fernndez, Rodrguez, L. de Santiago Rodrigo, and et al., "Coding Pronys method in MATLAB and applying it to biomedical signal filtering," *BMC Bioinformatics*, vol. 451, no. 19, 2018.

[17] J. K. Hwang, "Modal identification by curve-fiting of power spectra," in *2015 IEEE PES Asia-Pacific Power and Energy Engineering Conference (APPEEC)*, pp. 1–5, 2015.
[18] J. Khazaei, L. Fan, W. Jiang, and D. Manjure, "Distributed Prony analysis for real-world PMU data," *Electric Power Systems Research*, vol. 133, pp. 113 – 120, 2016.
[19] T. Xia, Y. Zhang, and et al, "Phase anglebased power system interarea oscillation detection and modal analysis," *European Transactions on Electrical Power*, vol. 21, no. 4, pp. 1629 – 1639, 2011.
[20] Y. Zhang, *Design of wide-area damping control systems for power system low-frequency inter-area oscillations*. Washington State University, 2007.
[21] W. Qiu, Q. Tang, and et al, "Multi-view convolutional neural network for data spoofing cyber-attack detection in distribution synchrophasors," *IEEE Transactions on Smart Grid*, vol. 11, no. 4, pp. 3457–3468, 2020.
[22] NERC, "Interconnection oscillation analysis: Reliability assessment," *North American Electric Reliability Corporation*, pp. 1–53, 2019.
[23] J. K. Hwang and Y. Liu, "Identification of interarea modes from ringdown data by curve-fitting in the frequency domain," *IEEE Transactions on Power Systems*, vol. 32, no. 2, pp. 842–851, 2017.

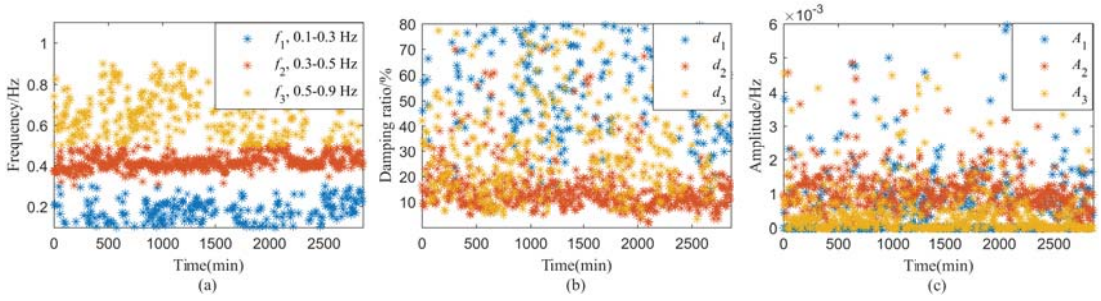

Fig. 8. The oscillation results of the ambient data in unit 634. (a)Frequency, the means of f_1, f_2, f_3 are 0.241, 0.407, and 0.735 Hz, respectively. The standard deviation are 0.024, 0.036, and 0.12. (b)Damping ratio, the means of f_1, f_2, f_3 are 25.75%, 21.83%, and 54.06%, respectively. The standard deviation are 0.156, 0.119, and 0.263. (c)Amplitude, the means of f_1, f_2, f_3 are 0.00150, 0.00137, and 0.000252 Hz, respectively.

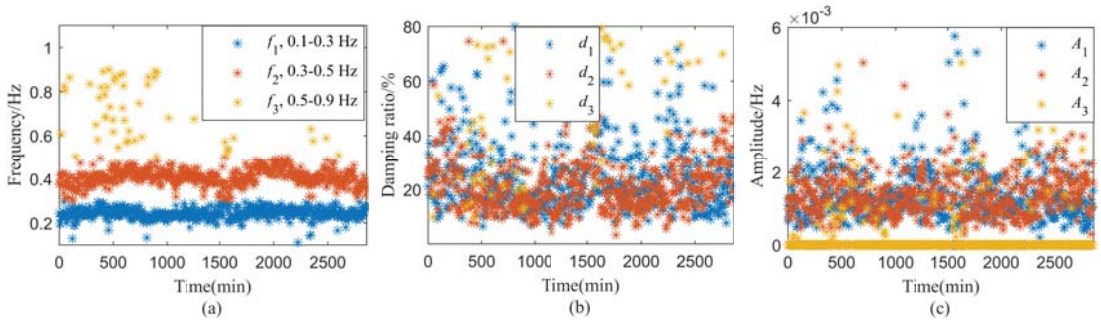

Fig. 9. The oscillation results of the ambient data in unit 686. (a)Frequency, the means of f_1, f_2, f_3 are 0.187, 0.421, and 0.669 Hz, respectively. The standard deviation are 0.053, 0.036, and 0.110. (b)Damping ratio, the means of f_1, f_2, f_3 are 40.14%, 17.20%, and 30.58%, respectively. The standard deviation are 0.195, 0.131, and 0.193. (c)Amplitude, the means of f_1, f_2, f_3 are 0.000625, 0.00112, and 0.000461 Hz, respectively.

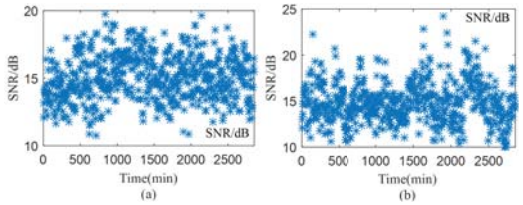

Fig. 10. The SNR of units 634 and 686. (a) SNR of unit 634, (b) SNR of unit 686.